



# Effects of microRNA-195 on the Prognosis of Glioma Patients and the Proliferation and Apoptosis of Human Glioma Cells

Ying Jia<sup>1</sup> · Ye Tian<sup>1</sup> · Shuo An<sup>1</sup> · Dong Yang<sup>2</sup>

Received: 21 October 2018 / Accepted: 19 February 2019 / Published online: 26 February 2019  
© Arányi Lajos Foundation 2019

## Abstract

Glioma is the most common and aggressive intracranial malignant tumor with poor prognosis. Acts as a tumor suppressor, microRNA-195 (miR-195) plays important roles in a variety of cancers. However, the expression of miR-195 and role of miR-195 in glioma are still not well understood. 186 patients with glioma were enrolled and the follow-up period ranges from 1 to 69 months. MiR-195 was exogenously transfected into human glioma U87 cell line. The cell proliferation assay (CCK-8), colony formation assay, cell cycle analysis and cell apoptosis analysis were examined to investigate miR-195 effect on U87 cells. MiR-195 levels were reversely correlated with pathological grades ( $r = -0.487$ ,  $p = 0.003$ ). For patients with low miR-195 levels, their median survival time was 15 months, whereas the median survival time in patients with high miR-195 levels was 56.53 months. Multi-factor Cox regression analysis showed that high level of miR-195 (Odds ratio (OR): 0.347, 95% CI: 0.121–0.992) was associated with decreased mortality risk of patients. Moreover, overexpression of miR-195 inhibits proliferation and colony formation, and induces apoptosis of U87 cells. MiR-195 could block the glioma cells in G0/G1 phase, reducing S phase cells and regulating apoptosis related proteins (Caspase-3, Caspase-8, Caspase-9 and Bcl-2). Downregulation of miR-195 was associated with poor prognosis in human glioma. MiR-195 acted as tumor suppressor through inhibiting cell proliferation and promoting cell apoptosis via blockade of cell cycle and regulation of apoptosis related proteins.

**Keywords** microRNA-195 · Glioma · Prognosis · Cell cycle · Cell proliferation · Apoptosis

## Introduction

Glioma is the most common and aggressive intracranial malignant tumor occurred in central nervous system. Glioma accounts for 75% of primary brain and other CNS tumors and 4% of children's tumors [1, 2]. Based on the newest cancer statistics, brain tumors are the leading cause of cancer death before age 40 years and in men and before age 20 years in women [3]. Glioma has high invasiveness, and there is often no clear boundary from the adjacent normal brain tissue. Therefore, it is difficult to eradicate through surgical treatment, and it is often easy to relapse and have high mortality.

With the progress of life science, the diagnosis and treatment of glioma is improving, but the prognosis of glioma patients is still remains poor [2, 3]. Thus, searching alternative approaches for glioma treatment is of great importance. Oncogenes or tumor suppressors play vital role in the development and progression of glioma, and some of them may serve as potential targets for glioma treatment.

MicroRNAs (miRs) are a class of non-coding RNAs, the length of miRs are approximately 22 nucleotides, which are highly conserved in the structure and function among different species [4, 5]. MicroRNAs are extensively involved in a variety of biological processes, such as cell proliferation, differentiation, apoptosis, cell cycle regulation, and angiogenesis [6–8]. Research has indicated that miRs play important roles in the development of glioma, involving in multiple process of tumorigenesis, such as invasion and angiogenesis [9].

MicroRNA-195 (miR-195) is an important member of miR-15, -16, -195, -424, and -497 families, plays variable roles in different diseases. In hypertrophic cardiomyopathy, miR-195 is highly expressed and could lead to myocardial cell growth disorder [10, 11]. Joglekar et al. indicated that miR-

✉ Dong Yang  
yangdong\_dr@163.com

<sup>1</sup> Department of Neurosurgery, Tianjin Medical University General Hospital, Tianjin 300052, China

<sup>2</sup> Department of Otorhinolaryngology, Tianjin Medical University General Hospital, No.154 An Shan Dao, Heping District, Tianjin 300052, China

195 could promote the regeneration of islet cells through Neurogenin3 in pancreas [12]. It has been reported that miR-195 act as a tumor suppressor and has been downregulated in a variety of cancers, such as hepatocellular carcinoma (HCC) [13], tongue squamous cell carcinoma (TSCC) [14], primary peritoneal carcinoma, bladder tumor, breast cancer and gastric carcinoma [15]. However, few reports mentioned the expression of miR-195 and its role in glioma.

In the present study, we aimed to study whether miR-195 expression is related to the pathological grades and prognosis of glioma patients. Besides, we also explore the role and underlying mechanism of miR-195 in cell proliferation and apoptosis in human glioma cells.

## Material and Methods

### Patients and Tissue Samples

186 patients with glioma were admitted to the Department of Neurosurgery of the Tianjin Medical University General Hospital from January 2012 to August 2017. All patients were first onset of glioma and surgical resection was performed. Pathologically confirmed tumor tissue samples and paired nontumorous tissues were collected and were snap-frozen in liquid nitrogen and stored at  $-70\text{ }^{\circ}\text{C}$  immediately. Pathological grading is classified based on the World Health Organization (WHO) classification of tumors for central nervous system (2010 edition) with grades I–IV, and also classified into astrocytic, oligodendrocytic or pilomyxoid tumors based on their histological characteristics. All patients were followed from the date of diagnosis to September 12, 2017. The follow-up period ranges from 1 to 69 months. Informed consent was obtained from all patients for using their samples and medical information. The study was approved by the Ethic Committee of Tianjin Medical University General Hospital.

### Cell Culture and miR-195 Transfection

Human glioma U87 cells was purchased from the Shanghai Cell bank of the Chinese Academy of Sciences (Shanghai, China). U87 cells were cultured in DMEM medium supplemented with 10% fetal bovine serum (FBS), 100 U/ml penicillin and 100  $\mu\text{g}/\text{ml}$  streptomycin. Cultures were incubated at  $37\text{ }^{\circ}\text{C}$  with 5%  $\text{CO}_2$ . MiR-195 mimics were RNA duplex designed and synthesized by Gene Company Ltd. (Shanghai, China). The negative control (NC) RNA duplex was non-homologous to any human genome sequences. miR-195 mimics sequence 5'-UAGCAGCACAGAAAUAUUGGC -3', was a 2'-O-methyl-modified oligoribonucleotide. The NC sequence,

was 5'-UCACAACCUCCUAGAAAGAGUAGA -3'. Lipofectamine 2000 Reagent (Invitrogen) was used for all transfection studies by following the manufacturer's protocol. RNA mimics (20 nM, 30 nM, 50 nM and 100 nM) and its negative controls were used. The transfection efficiency was determined using qRT-PCR. Briefly, total RNA was extracted from U187 cells using Trizol reagent (Life Technologies, Inc., USA), according to the manufacturer's instructions; 10  $\mu\text{g}$  of RNA was reverse-transcribed by a reverse transcription kit (ReverTra Ace R qPCR RT Kit (Toyobo Inc., Japan) from each group to obtain the corresponding cDNA. RT-qPCR was performed using the THUNDERBIRD R qPCR Mix (Toyobo Inc., Japan) on an ABI Prism 7900 sequence detection system (Applied Biosystems, CA, USA).  $\Delta\text{Ct}$  was normalized to the internal reference gene, RNU6B. The TaqMan PCR assay kit for miR-195 was purchased from Applied Biosystems, and the primer sequences used are as follows: forward primer was 5' GTCCATCTCCAGTACAGTGTG', and reverse primer was 5' AGCCATCTTTACCAGACAGTGT 3'. The RNU6 forward primer was 5' GCTTGCTTCAGCAGCACATA 3', and reverse primer was 5' AAAAACATGGAACCTTCACG 3'. The fold change of expression was calculated as  $2^{\Delta\text{Ct (Treated - Untreated)}}$ . The primer sequences are listed in Table 1. The qPCR cycle conditions were: one cycle of  $95\text{ }^{\circ}\text{C}$  for 30 s, 40 cycles of  $95\text{ }^{\circ}\text{C}$  for 15 s,  $60\text{ }^{\circ}\text{C}$  for 30 s, and  $72\text{ }^{\circ}\text{C}$  for 30 s. All the experiments were repeated three times to make it reliable.

### Cell Proliferation Assay

CCK-8 assay was used to detect cell proliferation. Briefly, U87 cells were divided into 3 groups, including blank (PBS), negative control group (transfected with 50 nm scrambled miRNAs) and miR-195 group (transfected with 50 nm miR-195 mimics). CCK-8 working solution was added 12 h, 24 h, 36 h, 48 h, 60 h and 72 h after transfection according to the manufacturer's instructions. After incubated for 1 h, absorbance at 450 nm was detected. The proliferation inhibiting rate was calculated as the following: Proliferation inhibiting rate =  $[\text{Absorbance (blank)} - \text{Absorbance (miR-195 or NC)}] / \text{Absorbance (blank)} \times 100\%$ .

### Colony Formation Assay

U87 cells were transfected with miRNA-195 mimics or scrambled miRNAs, respectively. After 48 h, cells were transferred into 6-well plates with a density of 1000 cells per well, and incubated for 10 days. Fresh complete medium was replaced every 3 days in the culture process. Then, the cell colonies were washed twice with and fixed with 3 ml methanol for 15 min. 1 ml/well of 0.1% crystal

**Table 1** The relationship between the patients' characteristics and prognosis

Factors	Patients (N)	Median survival (month)	One-year survival rate (%)	<i>P</i>
Sex				
Male	115	32.57	70.2 ± 8.2	0.207
Female	71	43.91	51.4 ± 11.2	
Age				
≤45	88	43	78.1 ± 9.5	0.094
>45	98	20	62.4 ± 9.7	
Radiotherapy\chemotherapy				
Yes	115	30	87.5 ± 6.12	0.024
No	71	12	44.1 ± 12.6	
Pathological grades				
Low	82	58.89	85.1 ± 7.5	0.002
High	104	23.53	56.6 ± 8.6	
Histologic Classification				
Astrocytoma	87	31.6	57.6 ± 7.1	0.025*
Oligodendroglioma	52	29.5	59.3 ± 6.4	0.014*
Pilocytic astrocytoma	40	59.32	86.2 ± 7.5	
IDH1/2 subclass				
Mutations	104	54.36	84.3 ± 8.2	0.015
Wild type	82	31.45	57.9 ± 7.4	
BRAF V600E subclass				0.027
Mutations	72	52.42	79.3 ± 7.6	
Wild type	114	33.12	59.4 ± 8.1	
miRNA-195				
Low	93	15	85.42 ± 6.9	0.003
High	93	56.53	61.81 ± 9.4	

*P* value was calculated for one-year survival rate by students' *t*-test;

\**P* < 0.05, compared with pilocytic astrocytoma. There is no significant difference on one-year survival rate between astrocytoma and oligodendroglioma

violet was added and incubated for 15 min, and then washed for 3 times using PBS. The number of cell clones was recorded and observed under the microscope.

### Flow Cytometric Analysis of Cell Cycle and Propidium Iodide DNA Staining

Effect of miR-195 on cell cycle was detected by flow cytometry (BD Accuri™ C6 Flow Cytometer, BD Biosciences, CA, USA). Briefly, cells were collected 48 h after transfection, and were fixed by freshly prepared 70% precooled alcohol overnight at 4 °C. Then, the cells were washed, filtrated and resuspend cells in 300–500 µl PI/Triton X-100 staining solution: to 10 ml of 0.1% (v/v) Triton X-100 (Sigma) in PBS and adding 0.40 ml of 500 µg/ml PI (Roche, USA). Stained with PI (propidium iodide) for 30 min at 4 °C. Incubate 37 °C for 15 min or for 30 min at 20 °C, then transfer tubes to ice or store at 4 °C protected from light. Acquire data on flow cytometer within 48 h. BD FACSDIVA™ software was used for data analysis.

### Acridine Orange/ Ethidium Bromide (AO/EB) Fluorescence Staining

Analysis of cell apoptosis and changes in cell morphology were evaluated using AO/EB fluorescence staining. Briefly, the suspension of NC-cells and miR-195-transfected cells, 4 µl/ml of dye mixture, containing 100 µg/ml acridine orange (Sigma, USA) and 100 µg/ml ethidium bromide (Sigma, USA) in PBS were added, and washed once with PBS. After staining, cells were visualized immediately under a fluorescence microscope (Nikon Eclipse Ti, Japan). The apoptotic cells were visualized with red color fluorescence. The apoptosis rate was calculated based on how many apoptotic cells per 100 cells, and ten random fields was selected for each slide.

### Caspase Activity

Aim to determine effect of miR-195 on enzyme activity of caspase family members, caspase 3, caspase 8 and caspase 9 had been selected to test their activity between miR-195-

transfected group and NC group. The commercial Caspase 3/8/9 Assay Kits had been purchased from abcam Biotechnology (CA, USA). All the procedure was followed the manual strictly. Taking caspase 3 activity assay as an example, the cell lysate from blank, NC and miR-195 transfected groups were used to test its inside caspase 3 activity. The assay is based on spectrophotometric detection of the chromophore p-nitroaniline (p-NA) after cleavage from the labeled substrate DEVD-pNA. The p-NA light emission can be quantified using a spectrophotometer or a microtiter plate reader at 400- or 405 nm. Comparison of the absorbance of p-NA from an apoptotic sample with an uninduced control allows determination of the fold increase in caspase 3 activity. Similar procedure was also performed on caspase 8 and caspase 9. The assays were performed in 96-well plate.

### Fluorescence Microscopy and Immunofluorescence Analysis of Bcl-2

The adherent U87 cells were mounted on slides. After washing in buffered saline, cells were fixed and permeabilized using the Dako intrastain kit (Tokyo, Japan). Monoclonal antihuman Bcl-2 antibody (Dako, Tokyo, Japan) were incubated at a 1/100 dilution in the dark at room temperature for 60 min, and second antibody Alexa Fluor® 568 (life technology, CA, USA) was added for another 30 min. Images captured using a Zeiss Axioskop fluorescent microscope in conjunction with Image Pro analysis software (Image pro Inc., USA). Random 10 field pictures were taken for each slide, and the average integrated optical density (IOD) of each filed was calculated to compare the BCL-2 expression among three groups.

### Statistical Analysis

Quantitative data with normal distribution were expressed as mean  $\pm$  standard deviation (SD); quantitative data which did not meet normal distribution requirements used median (interquartile range) for statistical description. Group comparison used student's *t* test or rank sum test. Categorical variable was described using percentage, and group comparison was done using chi square test or Fisher precision probability method. Correlation analysis was performed by Spearman rank correlation analysis. The time of the patient's diagnosis was observed as the starting point, death was the end point of the observation, and the survival period was recorded. Aim to thoroughly understand the association between miR-195 expression and survival, survival curves were analyzed by the stratified Kaplan-Meier method in the entire cohort, subgroup with pathological high grades and low grades, and subgroup with receiving chemotherapy separately; and the median miR-195 was used as threshold to divided patients into miR-195

high level group and low group in each cohort. The survival rate was compared with the Log-rank test. The multiple factor analysis was carried out by Cox regression in order to screen the meaningful covariate modeling. All data analysis was completed in SPSS 13.0 software. A probability value of  $P < 0.05$  was considered statistically significant.

## Results

### Clinical Characteristics of Patients

The demography of patients was listed in the Table 1. Among the 186 patients with glioma, 111 of them were male. The median age of first onset of glioma was  $45.35 \pm 15.42$  years, ranging from 15 to 81 years. 115 patients (61.8%) underwent chemotherapy; the other 71 patients (38.2%) did not receive radiotherapy and chemotherapy.

The 6-month survival rate was 73.4%, the one-year survival rate was 51.7%, and the two-year survival rate was 30.8%. The median survival time was 26 months (95% CI: 21.32–31.68 months). The histologic classification, pathological grades, and molecular subclasses of gliomas based on IDH1/2 mutants and BRAF mutants were also shown in Table 1.

### Relationship between miR-195 and Pathological Grades, Histological Types and Genotype Subgroups

The relationship between miR-195 and pathological grades of clinical glioma specimens was analyzed by Spearman rank correlation analysis. The results showed that miR-195 levels were reversely correlated with pathological grades ( $r = -0.487$ ,  $p = 0.003$ ). In patients with low pathological grades (grade I and II), the expression level of miR-195 was significantly higher than that in high pathological grades (grade III and IV) (Table 2). As for the histological classification, there is no significant difference on miR-195 level between astrocytoma and oligodendroglioma, but miR-195 from pilocytic astrocytoma is significantly higher than the other two histological types of gliomas. On the other hand, miR-195 levels from genotype subgroups with IDH1/2 mutation and BRAF<sup>VE600</sup> mutations, were significantly higher than wild-type subgroups (Table 2).

### MiR-195 and Prognosis of Patients

The median survival time and the 1-year survival rate were estimated by Kaplan-Meier method according to the patients' gender, age, pathological results and miRNA-195. The results of Log-rank test were shown in Table 1. Our results showed that acceptance of radiotherapy/chemotherapy, pathological grades and miRNA-195 are significantly associated with

**Table 2** The relationship between pathological grading and miR-195 expression

Subtype of gliomas	miRNA-195 level	<i>p</i>
Pathological grading		
Low	2.33 (1.97–2.81)	0.0074
High	0.89 (0.53–1.55)	
Histologic Classification		
Astrocytoma	0.94 (0.51–1.65)	0.0056*
Oligodendroglioma	0.85 (0.47–1.52)	0.0105*
Pilocytic astrocytoma	2.54 (1.99–2.94)	
IDH1/2 subclass		
Mutations	2.15 (0.68–2.36)	0.0245
Wild type	1.02 (0.54–1.99)	
BRAF V600E subclass		
Mutations	2.45 (2.01–2.97)	0.0184
Wild type	1.12 (0.58–2.03)	

Data was shown as median (interquartile range)

\*Compared with Pilocytic astrocytoma

prognosis of patients. The median survival time of patients who underwent radiotherapy\chemotherapy was 30 months, whereas the median survival time of patients who did not receive underwent radiotherapy\chemotherapy was only 12 months. The median survival time of patients with low pathological grades was 58.89 months; while that of patients with high pathological grades was 23.53 months. The median survival time of patients with low miR-195 levels was 15 months, whereas that with high miR-195 levels was 56.53 months. Survival analysis and association with miR-195 was conducted using the entire cohort was shown in Fig. 1a, and miR-195 effect on survival in the cohort with low grades and high grades was shown in Fig. 1b. Results demonstrated that cohort with high miR-195 levels had significantly longer survival time than miR-195 lower cohort.

Total 115 cases received chemotherapy and radiotherapy. In this subgroup, most patients belonged to high pathological grading. The median value of miR-195 was used as threshold to divide this cohort into miR-195 high group and miR-195 low group. And as shown in Fig. 1d, patients with higher miR-195 level also had long time survival time compared with lower miR-195 patients.

The association of relative factor with prognosis was further analyzed using multi-factor Cox regression analysis. As shown in Table 3, high level of miR-195 (OR: 0.359, 95% CI: 0.129–0.962), radiotherapy\chemotherapy (OR: 0.374, 95% CI: 0.149–0.974), IDH1/2 Mutation (OR: 0.676, 95% CI: 0.204–1.314), and pilocytic astrocytoma (OR: 0.533, 95% CI: 0.186–1.081) were associated with decreased mortality risk; while high pathological grades (OR: 3.147, 95% CI: 1.118–10.11) were associated with increased mortality risk of patients.

## Overexpression of miR-195 Inhibits Proliferation of U87 Cells

To overexpress miR-195 in glioma U87 cells, we transfected miR-195 mimics at concentrations of 20 nM, 30 nM, 50 nM and 100 nM, and the level of miR-195 was detected using real-time PCR. As shown in Fig. 2a, the expression level of miR-195 was significantly increased for about 6 times after transfection with 50 nM and 100 nM miR-195 mimics ( $F = 107.2$ ,  $p < 0.001$ ). Considering that the expression levels are similar after transfection with 50 nM and 100 nM miR-195 mimics, we chose 50 nM as the transfection concentration for following experiments.

Then we detect the effect of miR-195 on cell growth of U87 cells using CCK-8 assay. Cell Counting Kit-8 (CCK-8) was used detect cell growth 12, 24, 36, 48, 60 and 72 h after transfection with 50 nM miR-195 mimics or miRNA negative control. Inhibition rate at each timepoint was calculated as follows:

Proliferation inhibiting rate =

$$\frac{[\text{Absorbance (blank)} - \text{Absorbance (miR-195 or NC)}]}{\text{Absorbance (blank)}} \times 100\%.$$

We found that the overexpression of miR-195 could inhibit cell proliferation. The maximum inhibitory rate of cell growth occurred at 48 h after transfection ( $p < 0.001$ , Fig. 2b).

## Effect of miR-195 on Cell Cycle

In order to further analyze whether miR-195 inhibit cell proliferation through regulating cell cycle, we detected cell cycle distribution of different experimental groups by flow cytometry. Our data showed that cells were significantly arrested in G0/G1 phase in the miR-195 group, and the number of cells at S phase was significantly decreased, as compared with the NC and blank groups ( $p < 0.05$ , Fig. 3 and Table 4). The results indicate that miR-195 could significantly inhibit cell proliferation through blocking the glioma cells in G0/G1 phase and reduce S phase cells.

## Overexpression of miR-195 Inhibits Colony Formation of U87 Cells

The colony formation of U87 cells after transfection of miR-195 was detected using colony formation assay. The results showed that there were significant differences regarding the number of colonies in the Blank group ( $445 \pm 31$ ), NC (negative control) group ( $459 \pm 29$ ), and miR-

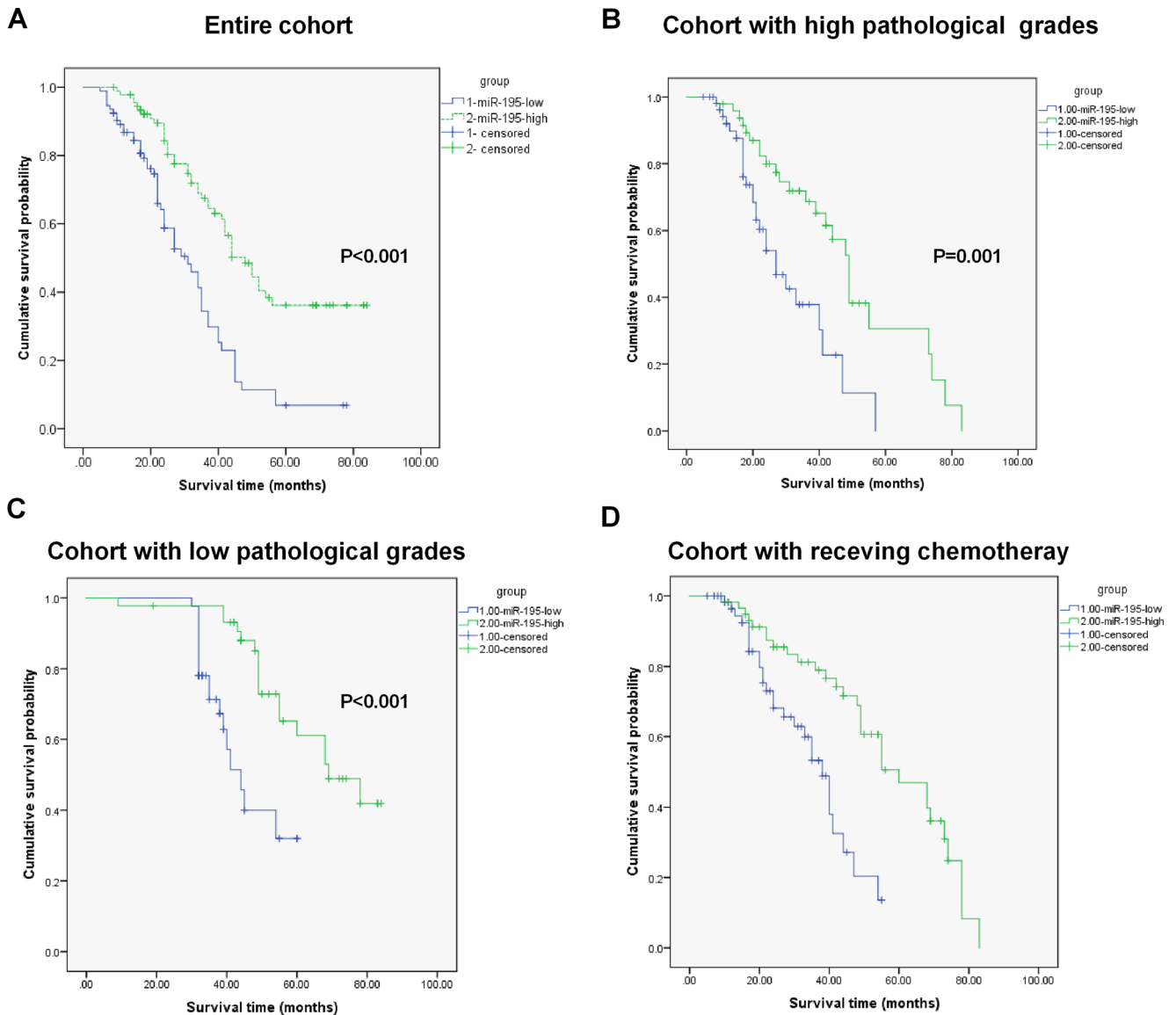


**Fig. 1** Cumulative survival curve of glioma patients with low level of miR-195 or with high level of miR-195. **a** entire cohort; **b** sub-cohort with high grades; **c** sub-cohort with low grades; **d** sub-cohort with receiving chemotherapy and radiotherapy

195 group ( $301 \pm 21$ ) ( $F = 44.21, p < 0.001$ ). The number of colonies in the miR-195 group was significantly

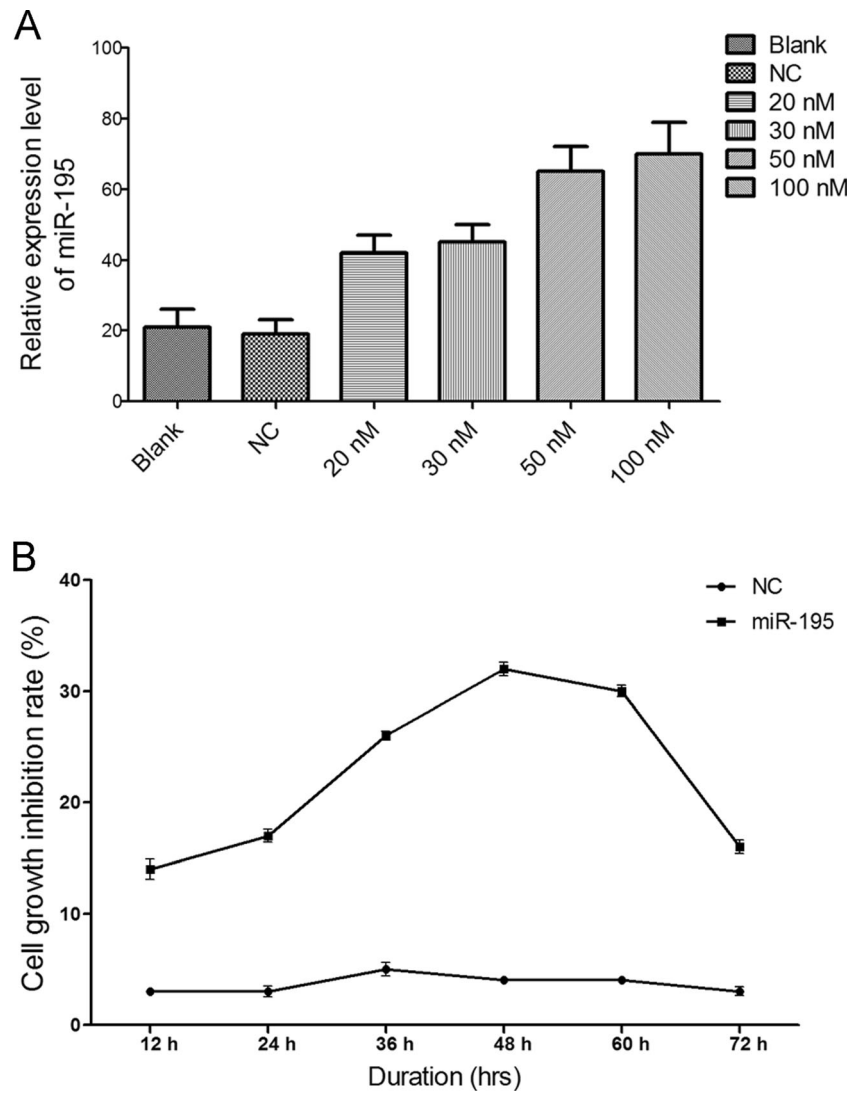
decreased than that in the Blank group and NC group ( $p < 0.05$ , Fig. 4 and Table 5).

**Table 3** Multi-factor Cox regression analysis

Variables	OR	95% confidence interval (CI)	P
High miRNA-195	0.347	0.121–0.992	0.045
High Pathological grades	2.688	1.014–8.245	0.029
Radiotherapy\chemotherapy (Yes vs No)	0.425	0.171–1.102	0.046
Histologic Classification (Pilocytic vs. others)	0.533	0.186–1.081	0.031
IDH1/2 Mutation	0.676	0.204–1.314	0.037
BRAF V600E Mutation	0.751	0.345–1.553	0.051

OR odds ratio

**Fig. 2** Overexpression of miR-195 inhibits proliferation of U87 cells. **a** The level of miR-195 was detected using real-time PCR after transfection of miR-195 mimics at concentrations of 20 nM, 30 nM, 50 nM and 100 nM. U6 was used as an endogenous control. **b** The effect of miR-195 on cell growth of U87 cells using CCK-8 assay. Cell Counting Kit-8 (CCK-8) was used to detect cell growth 12, 24, 36, 48, 60 and 72 h after transfection with 50 nM miR-195 mimics or miRNA negative control. Proliferation inhibiting rate = [Absorbance (blank) - Absorbance (miR-195 or NC)] / Absorbance (blank) × 100%



**Overexpression of miR-195 Promotes Apoptosis of U87 Cells by Targeting Caspase Family Members and BCL-2**

The morphological changes of the U87 cells-transfected with miR-195 was analyzed by acridine orange/ethidium bromide

(AO/EB) fluorescence staining. AO/EB staining showed a concentration-dependent increase of apoptosis on miR-195 transfected cells, relative to the negative control. Cells stained green are viable cells, whereas, orange/red dots of condensed nuclei were of apoptosis. Cells transfected with miR-195 exhibited characteristic changes of apoptosis e.g. cell shrinkage,

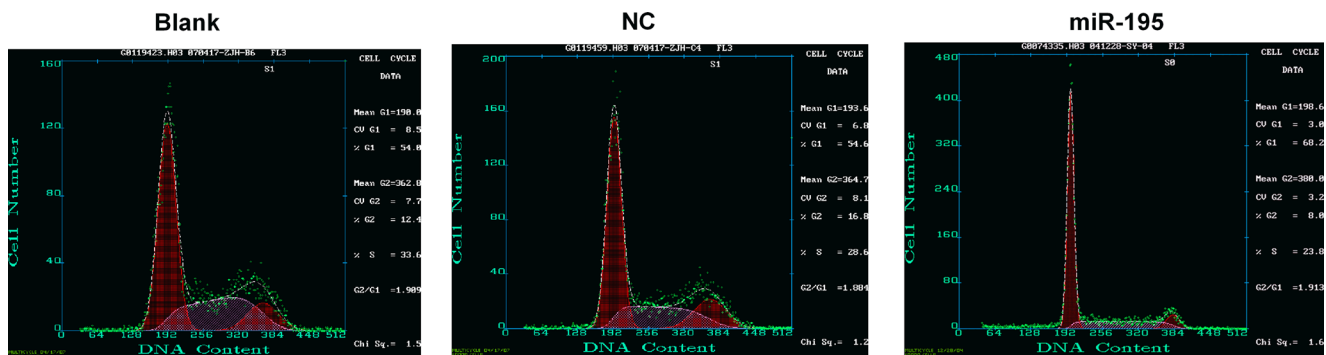


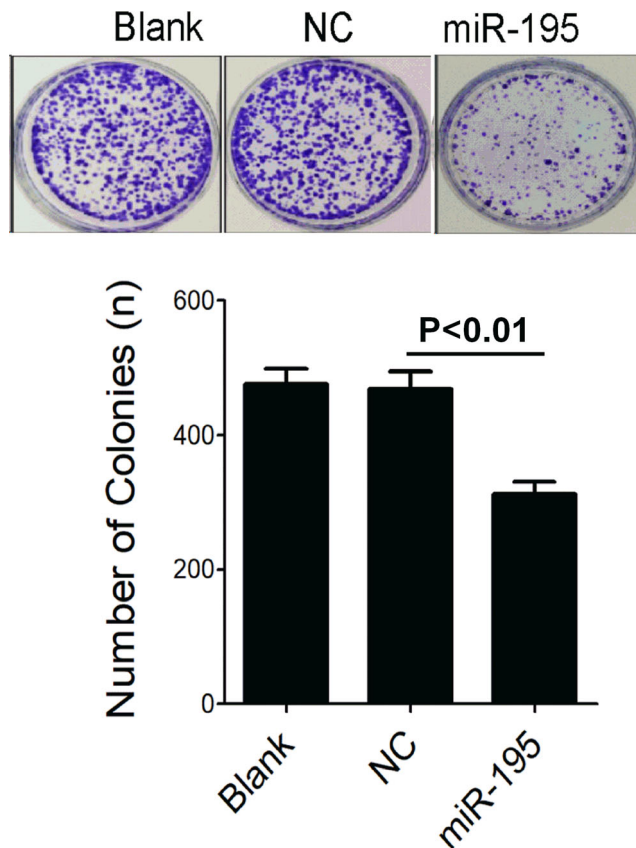
**Fig. 3** Overexpression of miR-195 inhibits colony formation. The colony formation of U87 cells after transfection of miR-195 was detected using colony formation assay

**Table 4** Effect of miR-195 on cell cycle of U87

Group	Blank	NC	miR-195	P
G0/G1	0.51 ± 0.042	0.51 ± 0.041	0.695 ± 0.036	0.033
S	0.262 ± 0.025	0.248 ± 0.035	0.161 ± 0.038	0.020
G2/M	0.197 ± 0.029	0.201 ± 0.029	0.144 ± 0.038	0.814

nuclear condensation, fragmentation and formation of apoptotic bodies. (Fig. 5a). On the other hand, cells transfected with negative control vector did not shown visible apoptotic characteristics.

We further detected the effect of overexpression of miR-195 on Bcl-2, Caspase-3, Caspase-8, and Caspase-9. As shown in Fig. 5b, by immunofluorescence, the level of Bcl-2 was significantly decreased after overexpression of miR-195 in glioma U87 cells compared with NC group (Fig. 5b). Moreover, overexpression of miR-195 could also significantly increase the activity of Caspase-3 and Caspase-9 in U87 cells ( $p < 0.001$ ); while there was no significantly changes on the activity of Caspase-8 (Table 6).

**Fig. 4** Cell cycle distribution by flow cytometry. miR-195 significantly blocks the cell cycle in G0/G1 phase in U87 cells**Table 5** Comparison of apoptosis rate in the Bland, NC and miR-195 group

Group	Apoptosis rate (%)	F	p
Blank	3.80 ± 0.72	558.62	<0.001
NC	5.92 ± 0.81		
miR-195	27.1 ± 2.1*		

\*  $P < 0.05$ , as compared with NC group

## Discussions

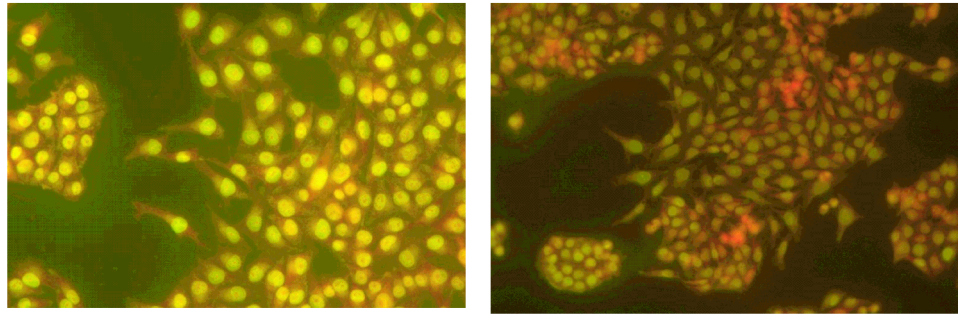
In the present study, we found that miR-195 levels were reversely correlated with pathological grades in 186 patients with glioma. Moreover, the median survival time was longer in patients with high miR-195 levels than those in low miR-195 levels. Multi-factor Cox regression analysis revealed that high level of miR-195 (OR: 0.363, 95% CI: 0.135–0.975) was associated with decreased mortality risk in patients with glioma. We further investigated the underlying mechanism in glioma U87 cells. The results showed that overexpression of miR-195 could inhibit the proliferation and colony formation, and promote apoptosis of U87 cells. The role of miR-195 on cell proliferation and apoptosis may function through blocking the glioma cells in G0/G1 phase, reducing S phase cells and regulating apoptosis related proteins (Caspase-3, Caspase-8, Caspase-9 and Bcl-2).

Soon and colleges [16] found that the expression level of miR-195 was significantly lower in patients with adrenocortical carcinoma than that in adrenocortical adenomas. Their results also indicated that downregulation of miR-195 was significantly associated with poorer disease-specific survival in adrenocortical carcinomas using Kaplan-Meier analysis. Wang et al. [17] reported that decrease of miR-195 in HCC tissues was significantly associated with worse recurrence-free survival. In another study, Lakomy and colleges assessed 38 patients with glioblastoma multiforme (GBM), and found that miR-195 was positively correlated with overall survival [18]. Interestingly, Ilhan-Mutlu et al. [19] reported that expression level of miR-195 did not significantly differ after comparing the initial and recurrent glioblastoma specimens in 15 primary glioblastoma patients. Their results revealed a stable expression of miR-195 in glioblastoma which might be useful as biomarkers or therapeutic targets in tumor entity.

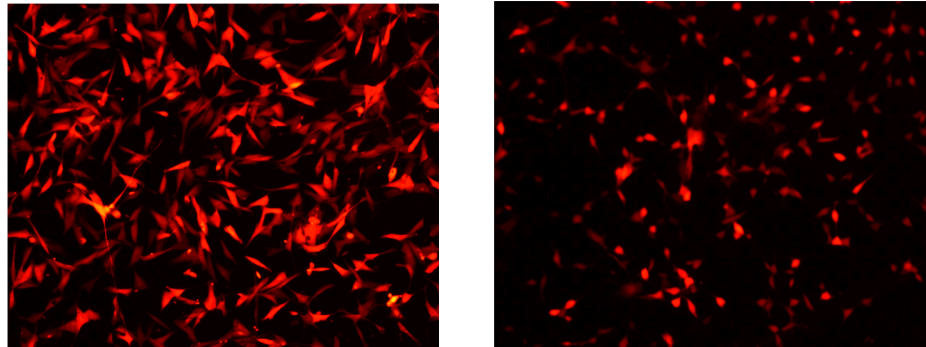
In the study, we found that miR-195 was significantly reversely correlated with pathological grades in 186 patients with glioma. Moreover, miR-195 was positively associated with survival time. However, the results of this study are limited by the limited number of samples, incomplete clinical data, pathologists' subjectivity, and tumor heterogeneity. In the future, the clinical value of detecting miRNA-195 concentration of glioma tissues in predicting the prognosis of glioma patients could be further explored

**Fig. 5 Overexpression of miR-195 promotes apoptosis of U87 cells by targeting BCL2. a** AO/EB staining demonstrates that miR-195 overexpression could significantly induce the cell apoptosis; **b** The protein level of Bcl-2 in U87 cells is significantly in miR-195 transfected cells compared to NC group by immunofluorescence

### A AO/EB staining for apoptosis



### B Cell immunofluorescence for BCL2



using the screening and verification of large samples and in coupled with the maturity of the gene chip technology.

MiR-195, located on the chromosome 17p13.1, is considered to be a tumor suppressor gene. There are a large number of reports on the loss of 17q, 17p, 9p, and 13q chromosomes in glioma and cell lines, which cause the inactivation of the monitoring point in G1/S stage, the disorder of cell cycle regulation, the abnormal proliferation of cells, and the final formation of tumor. However, the role of miR-195 has been less reported in human glioma. It has been reported that the expression of miR-195 was obviously decreased in glioblastoma cell lines, as compared with normal brain tissues [20–22]. The overexpression of miR-195 in the glioblastoma cell line could obviously block the cell cycle and inhibit the invasion of the cells through E2F3 and CCND3 [20]. In our study, after overexpression of

miR-195, we found that cell proliferation was significantly inhibited, and the maximum inhibitory rate of cell growth occurred at 48 h after transfection. We further detected the effect of miR-195 on cell cycle by flow cytometry. The results indicated that miR-195 could block the glioma cells in G0/G1 phase, and reduce S phase cells.

Numerous studies have reported the role of miR-195 in promoting cell apoptosis of various types of cancers, such as human colorectal cancer, hepatocellular carcinoma, and breast cancer [23–26]. Similarly, we also found that miR-195 was able to promote apoptosis of glioma cells. Bcl-2 is one of the most important oncogene which plays vital role in cell apoptosis. The Bcl-2 protein family controls cell apoptosis mainly through regulating mitochondrial outer membrane permeabilization (MOMP) which cause the subsequent caspase activation, and apoptosis [27–29]. Bcl-2 is an identified target of miR-195 in previous literature. Zhu et al. reported that miR-195 could promotes palmitate-induced apoptosis through downregulate Bcl-2 in cardiomyocytes [30]. Liu et al. revealed a role of miR-195 in apoptosis inducing in human colorectal cancer cells via directly binding to the 3' UTR of Bcl-2 [24]. Here we found that overexpression of miR-195 could significantly inhibited the level of Bcl-2.

Caspases family belong to a highly conserved aspartate-specific cysteine proteases family, plays core roles in cell apoptosis [31]. The apoptotic caspases are composed of two-sub types, including initiator caspases and executioner caspases

**Table 6** Effect of miR-195 on the activity of Caspase-3, Caspase-8, and Caspase-9

Group	Blank	NC	miR-195	<i>P</i>
Caspase-3	0.155 ± 0.014	0.159 ± 0.014	0.484 ± 0.026*#	<0.001
Caspase-8	0.142 ± 0.021	0.168 ± 0.014	0.415 ± 0.019	<0.001
Caspase-9	0.166 ± 0.014	0.171 ± 0.017	0.179 ± 0.040*#	0.715

The data was shown as optical absorbance value at 405 nm

\* *P* < 0.05, as compared with the Blank group

# *P* < 0.05, as compared with the NC group

[32, 33]. Apoptotic signal first activates initiator caspases, followed by the activation of executioner caspases. Caspase-8 and caspase-9 are two typical initiator caspases, which mediate death receptor related signals and cytotoxic death signals, respectively. Activation of caspase-3 is necessary for cascade reaction of apoptotic proteases. In the present study, we found that overexpression of miR-195 could activated the caspase-3 and caspase-9; while caspase-8 was not activated. The data suggest that miR-195 promotes apoptosis of glioma cells through activating caspase-3 and caspase-9.

## Conclusion

Taken together, we found that downregulation of miR-195 was associated with poor prognosis in human glioma. MiR-195 acted as tumor suppressor through inhibiting cell proliferation and promoting cell apoptosis via blockade of cell cycle and regulation of apoptosis related proteins. MiR-195 may serve as a potential target for glioma treatment.

## Compliance with Ethical Standards

**Conflicts of Interest** All authors have no potential conflicts of interest.

**Publisher's Note** Springer Nature remains neutral with regard to jurisdictional claims in published maps and institutional affiliations.

## References

- Li K, Lu D, Guo Y, Wang C, Liu X, Liu Y, Liu D (2018) Trends and patterns of incidence of diffuse glioma in adults in the United States, 1973-2014. *Cancer Med* 7:5281–5290. <https://doi.org/10.1002/cam4.1757>
- Xia Z, Qiu D, Deng J, Jiao X, Yang R, Sun Z, Wan X, Li J (2018) Methylation-induced downregulation and tumor-suppressive role of microRNA-98 in glioma through targeting Sal-like protein 4. *Int J Mol Med* 41(5):2651–2659. <https://doi.org/10.3892/ijmm.2018.3464>
- Siegel RL, Miller KD, Jemal A (2018) Cancer statistics, 2018. *CA Cancer J Clin* 68(1):7–30. <https://doi.org/10.3322/caac.21442>
- Ahir BK, Ozer H, Engelhard HH, Lakka SS (2017) MicroRNAs in glioblastoma pathogenesis and therapy: a comprehensive review. *Crit Rev Oncol Hematol* 120:22–33. <https://doi.org/10.1016/j.critrevonc.2017.10.003>
- Barciszewska AM (2016) MicroRNAs as efficient biomarkers in high-grade gliomas. *Folia Neuropathol* 54(4):369–374. <https://doi.org/10.5114/fn.2016.64812>
- Bartel DP (2004) MicroRNAs: genomics, biogenesis, mechanism, and function. *Cell* 116(2):281–297
- Zhang F, Meng W, Tong B (2016) Down-regulation of MicroRNA-133b suppresses apoptosis of Lens epithelial cell by up-regulating BCL2L2 in age-related cataracts. *Med Sci Monit* 22:4139–4145
- Zhang Y, Peng Z, Zhao Y, Chen L (2016) microRNA-25 inhibits cell apoptosis of human gastric adenocarcinoma cell line AGS via regulating CCNE1 and MYC. *Med Sci Monit* 22:1415–1420
- Heneghan HM, Miller N, Lowery AJ, Sweeney KJ, Newell J, Kerin MJ (2010) Circulating microRNAs as novel minimally invasive biomarkers for breast cancer. *Ann Surg* 251(3):499–505. <https://doi.org/10.1097/SLA.0b013e3181cc939f>
- Chen H, Untiveros GM, McKee LA, Perez J, Li J, Antin PB, Konhilas JP (2012) Micro-RNA-195 and -451 regulate the LKB1/AMPK signaling axis by targeting MO25. *PLoS One* 7(7):e41574. <https://doi.org/10.1371/journal.pone.0041574>
- Busk PK, Cirera S (2010) MicroRNA profiling in early hypertrophic growth of the left ventricle in rats. *Biochem Biophys Res Commun* 396(4):989–993. <https://doi.org/10.1016/j.bbrc.2010.05.039>
- Joglekar MV, Parekh VS, Mehta S, Bhonde RR, Hardikar AA (2007) MicroRNA profiling of developing and regenerating pancreas reveal post-transcriptional regulation of neurogenin3. *Dev Biol* 311(2):603–612. <https://doi.org/10.1016/j.ydbio.2007.09.008>
- Yu S, Jing L, Yin XR, Wang MC, Chen YM, Guo Y, Nan KJ, Han LL (2017) MiR-195 suppresses the metastasis and epithelial-mesenchymal transition of hepatocellular carcinoma by inhibiting YAP. *Oncotarget* 8(59):99757–99771. <https://doi.org/10.18632/oncotarget.20909>
- Jia LF, Wei SB, Gong K, Gan YH, Yu GY (2013) Prognostic implications of microRNA miR-195 expression in human tongue squamous cell carcinoma. *PLoS One* 8(2):e56634. <https://doi.org/10.1371/journal.pone.0056634>
- Cecene G, Ak S, Eskiler GG, Demirdogen E, Erturk E, Gokgoz S, Polatkan V, Egeli U, Tunca B, Tezcan G, Topal U, Tolunay S, Tasdelen I (2016) Circulating miR-195 as a therapeutic biomarker in Turkish breast Cancer patients. *Asian Pac J Cancer Prev* 17(9):4241–4246
- Soon PS, Tacon LJ, Gill AJ, Bambach CP, Sywak MS, Campbell PR, Yeh MW, Wong SG, Clifton-Bligh RJ, Robinson BG, Sidhu SB (2009) miR-195 and miR-483-5p identified as predictors of poor prognosis in adrenocortical Cancer. *Clin Cancer Res* 15(24):7684–7692. <https://doi.org/10.1158/1078-0432.CCR-09-1587>
- Wang R, Zhao N, Li S, Fang JH, Chen MX, Yang J, Jia WH, Yuan Y, Zhuang SM (2013) MicroRNA-195 suppresses angiogenesis and metastasis of hepatocellular carcinoma by inhibiting the expression of VEGF, VAV2, and CDC42. *Hepatology* 58(2):642–653. <https://doi.org/10.1002/hep.26373>
- Lakomy R, Sana J, Hankeova S, Fadrus P, Kren L, Lzicarova E, Svoboda M, Dolezelova H, Smrcka M, Vyzula R, Michalek J, Hajdich M, Slaby O (2011) MiR-195, miR-196b, miR-181c, miR-21 expression levels and O-6-methylguanine-DNA methyltransferase methylation status are associated with clinical outcome in glioblastoma patients. *Cancer Sci* 102(12):2186–2190. <https://doi.org/10.1111/j.1349-7006.2011.02092.x>
- Ilhan-Mutlu A, Wohrer A, Berghoff AS, Widhalm G, Marosi C, Wagner L, Preusser M (2013) Comparison of microRNA expression levels between initial and recurrent glioblastoma specimens. *J Neuro-Oncol* 112(3):347–354. <https://doi.org/10.1007/s11060-013-1078-6>
- Zhang QQ, Xu H, Huang MB, Ma LM, Huang QJ, Yao Q, Zhou H, Qu LH (2012) MicroRNA-195 plays a tumor-suppressor role in human glioblastoma cells by targeting signaling pathways involved in cellular proliferation and invasion. *Neuro-Oncology* 14(3):278–287. <https://doi.org/10.1093/neuonc/nor216>
- Gaur A, Jewell DA, Liang Y, Ridzon D, Moore JH, Chen C, Ambros VR, Israel MA (2007) Characterization of microRNA expression levels and their biological correlates in human cancer cell lines. *Cancer Res* 67(6):2456–2468. <https://doi.org/10.1158/0008-5472.CAN-06-2698>
- Henriksen M, Johnsen KB, Olesen P, Pilgaard L, Duroux M (2014) MicroRNA expression signatures and their correlation with clinicopathological features in glioblastoma multiforme. *NeuroMolecular Med* 16(3):565–577. <https://doi.org/10.1007/s12017-014-8309-7>
- Wang A, Ren M, Song Y, Wang X, Wang Q, Yang Q, Liu H, Du Z, Zhang G, Wang J (2018) MicroRNA expression profiling of bone marrow mesenchymal stem cells in steroid-induced osteonecrosis

- of the femoral head associated with osteogenesis. *Med Sci Monit* 24:1813–1825
24. Liu L, Chen L, Xu Y, Li R, Du X (2010) microRNA-195 promotes apoptosis and suppresses tumorigenicity of human colorectal cancer cells. *Biochem Biophys Res Commun* 400(2):236–240. <https://doi.org/10.1016/j.bbrc.2010.08.046>
  25. Li C, Zhao Q, Zhang W, Chen M, Ju W, Wu L, Han M, Ma Y, Zhu X, Wang D, Guo Z, He X (2017) MicroRNA-146b-5p identified in porcine liver donation model is associated with early allograft dysfunction in human liver transplantation. *Med Sci Monit* 23:5876–5884
  26. Yu M, Zhang X, Li H, Zhang P, Dong W (2017) MicroRNA-588 is downregulated and may have prognostic and functional roles in human breast cancer. *Med Sci Monit* 23:5690–5696
  27. Li F, Liang A, Lv Y, Liu G, Jiang A, Liu P (2017) MicroRNA-200c inhibits epithelial-mesenchymal transition by targeting the BMI-1 gene through the Phospho-AKT pathway in endometrial carcinoma cells in vitro. *Med Sci Monit* 23:5139–5149
  28. Tian Z, Zhou H, Xu Y, Bai J (2017) MicroRNA-495 inhibits new bone regeneration via targeting high mobility group AT-hook 2 (HMGA2). *Med Sci Monit* 23:4689–4698
  29. Zhang Z, Li H, Chen S, Li Y, Cui Z, Ma J (2017) Knockdown of MicroRNA-122 protects H9c2 cardiomyocytes from hypoxia-induced apoptosis and promotes autophagy. *Med Sci Monit* 23:4284–4290
  30. Fang DZ, Wang YP, Liu J, Hui XB, Wang XD, Chen X, Liu D (2018) MicroRNA-129-3p suppresses tumor growth by targeting E2F5 in glioblastoma. *Eur Rev Med Pharmacol Sci* 22(4):1044–1050. [https://doi.org/10.26355/eurev\\_201802\\_14387](https://doi.org/10.26355/eurev_201802_14387)
  31. Szemraj M, Oszejca K, Szemraj J, Jurowski P (2017) MicroRNA expression analysis in serum of patients with congenital hemochromatosis and age-related macular degeneration (AMD). *Med Sci Monit* 23:4050–4060
  32. Zhang J, Qin L, Han L, Zhao Y, Jing H, Song W, Shi H (2017) Role of MicroRNA-93 I in pathogenesis of left ventricular remodeling via targeting cyclin-D1. *Med Sci Monit* 23:3981–3988
  33. Gan TQ, Chen WJ, Qin H, Huang SN, Yang LH, Fang YY, Pan LJ, Li ZY, Chen G (2017) Clinical value and prospective pathway signaling of MicroRNA-375 in lung adenocarcinoma: a study based on the Cancer genome atlas (TCGA), gene expression omnibus (GEO) and bioinformatics analysis. *Med Sci Monit* 23:2453–2464